Scanning Tunneling Microscopy and Scanning Tunneling Spectroscopy Studies of Planar and Nonplanar Naphthalocyanine on Graphite (0001). Part 2: Tip−Sample Distance-Dependent *I*−*V* Spectroscopy

Thiruvancheril G. Gopakumar,* Falk Müller, and Michael Hietschold*

Chemnitz University of Technology, Institute of Physics, Solid Surfaces Analysis Group, D-09107 Chemnitz, Germany

Received: September 28, 2005; In Final Form: January 1, 2006

Tip−sample distance-dependent current−voltage tunneling spectroscopy on monolayers of base-free naphthalocyanine (Nc), a planar molecule, and tin−naphthalocyanine (SnNc), a nonplanar molecule, has been studied on a freshly cleaved highly oriented pyrolytic graphite (HOPG) surface using a variable-temperature STM at 50 K under ultra-high vacuum conditions. The current−voltage curves show an unsymmetrical diode-like nature especially at large tip−sample distances in both cases. Normalized differential conductivity of all spectra has been considered for further analysis. The ionization and electron affinity levels are compared with the single-molecule local density of states (LDOS) near the Fermi energy using a theoretical calculation for Nc and SnNc. A tip−sample distance-dependent highest occupied molecular orbital−lowest unoccupied molecular orbital (HOMO−LUMO) gap shrinking is observed in the case of Nc, in which the filled levels of the molecules are pinned while the unfilled levels near the Fermi energy are shifting toward lower energy. In contrast, there is no such HOMO−LUMO gap shrinking in the case of the SnNc decreasing tip−sample distance. However, a subsequent increase in the tunneling current was observed by almost 1 order of magnitude compared with Nc. A model is proposed to explain this phenomenon where the Nc−graphite interface is considered as a pure capacitive interface.

Introduction

This article is the continuation of the previous one, in which we discussed the adsorption geometry of the planar and nonplanar naphthalocyanines and the influence of the geometry on the adlayer structure. The present part deals with the spectroscopic studies of the same systems, especially the orbital-mediated tunneling and the tip−sample distance-dependent current−voltage characteristics.

Multiple quantum well structures based on organic semiconductors have found increasing attention due to interesting effects such as the tunable density of conduction and valence band states,[1] the quantum-confined Stark effect,[2] and some nonlinear optical phenomena.[3,4] In the existing varieties of organic semiconductors, phthalocyanines (Pc) are an interesting class which has already shown different applications especially in light-emitting diodes, organic field effect transistors, sensors, solar cells, and so forth.[5−8] Understanding the electronic and spectroscopic properties of these molecules is extremely important when a technology based on these systems is concerned.

The scanning tunneling microscope (STM) is a versatile tool, which provides the opportunity to perform local spectroscopy of occupied and unoccupied states of molecular systems adsorbed on different conducting substrates. The energy gap between the highest occupied molecular orbital (HOMO) and the lowest unoccupied molecular orbital (LUMO) has been measured for different Pcs using STM. Barlow and Hipps have investigated the energy gap of VOPc using orbital-mediated tunneling spectroscopy.[9] Our group has performed similar investigations on SnPc[10] and Nc[11] using scanning tunneling spectroscopy. Charge-carrier injection into CuPc thin films was studied by Alvarado et al. who have shown the so-called single-particle band gap of CuPc.[12] Hipps et al. studied the orbital-mediated tunneling spectrum and resonant tunneling in different metal phthalocyanines.[13−15] Ho et al. have studied the electron transport through single CuPc molecules, and from the differential conductance spectra, they elucidated the vibronic states of individual molecules.[16]

However, in the above-mentioned reports, the tip−sample distance-dependent orbital-mediated tunneling, influence of the tip on the tunneling states, and the tip−sample interactions have rarely been considered. Deng and Hipps studied the tip−sample distance-dependent tunneling spectra for Ni(II) tetraphenylporphyrin adsorbed on Au(111) where they found no effect of the tip on the molecular layers (no measurable changes in orbital energy splitting). However, a tip-induced charging and thus a shift in the energy states were predicted in this case.[17] McEllistrem et al. studied the electrostatic tip−sample interaction in the STM on different n-type silicon surfaces, in which they concluded that the pinned surfaces can become unpinned by the tip−sample interaction.[18] Feenstra concluded that a tip-induced band bending due to the high local electric field between the tip and sample might result in spectral shifts of several tenths of an electronvolt for the electronic states of semiconductors.[19] Müller et al. have shown a distance-dependent work function change in the case of Pt−Au and W−Pt tip−sample systems.[20] The tip−sample distance-dependent tunneling spectrum in the case of molecular systems adsorbed on different substrates is still of considerable interest from a fundamental and techno-

* To whom correspondence should be addressed. Fax: +49 371 531 3181. E-mail: thiruvacheril.gopakumar@physik.tu-chemnitz.de (T.G.G.). Fax: +49 371 531 3181. E-mail: hietschold@physik.tu-chemnitz.de (M.H.).

10.1021/jp055535z CCC: $33.50
Published on Web 02/24/2006

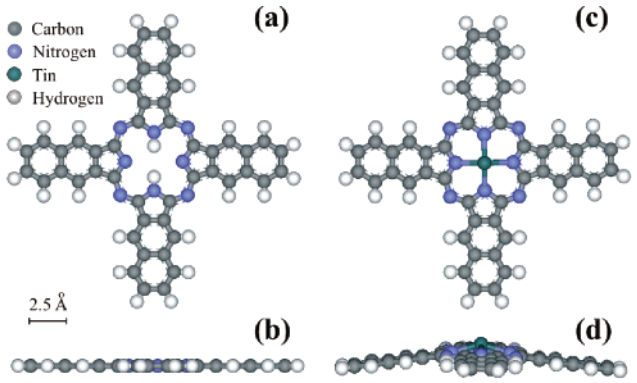

Figure 1. Energy-optimized geometric structure: (a) and (b) show the front and side views of Nc and (c) and (d) show the front and side views of SnNc. In both side views, one of the molecular axes is perpendicular to the plane of the paper.

logical perspective. Here, we study the distance-dependent current−voltage ($I-V$) spectroscopy of base-free naphthalocyanine (planar) and tin−naphthalocyanine (nonplanar) on a comparatively weak interacting substrate as highly oriented pyrolytic graphite (HOPG). Normalized differential conductivity−voltage curves are compared with the calculated local density of states (LDOS), and the peak positions are assigned to the corresponding filled and unfilled levels.

Experimental Section

Nc and SnNc have been purchased with a purity of 95% from Aldrich and later cleaned by several cycles of heating in high vacuum and then in ultra-high vacuum (UHV). The monolayer is prepared by organic molecular beam epitaxy (OMBE) in which the molecules are heated to their evaporation temperature by resistive heating in a Knudsen cell (K-cell). This kind of deposition gives a stable rate of evaporation which is further controlled by a previously calibrated quartz microbalance and by subsequent in-situ STM and low-energy electron diffraction (LEED) measurements. During the deposition, samples are held at room temperature at a background pressure of around 10^{-10} mbar. The deposition rate measured by a quartz crystal microbalance is approximately 0.1 nm/min for 8 min from previously degassed molecules. Graphite has been freshly cleaved and annealed at 550 °C for 12 h prior to deposition. Electrochemically etched tungsten tips have been used for the investigation, and all tips have been cleaned by subsequent Ar^+-ion sputtering and several heating cycles up to 700 °C. Experiments have been carried out at a sample temperature of 50 K using a VT-STM from Omicron equipped with sample cooling by a liquid helium flow cryostat. During the spectroscopic measurements ($I-V$), the feedback loop was kept off. The spectra have been recorded with 100 data points for an acquisition time of 100 μs and a delay of 50 μs. The normalized differential conductivity has been obtained by dividing the smoothened first derivative of the $I-V$ curves, dI/dV, with smoothened $I-V$ curves. The smoothening has been performed in this case to avoid artificial mathematical errors produced in the normalized differential conductivity.

Results

The energy-optimized geometrical structures of both Nc and SnNc calculated using B3LYP by Gaussian 03 are shown in Figure 1. Parts a and b of Figure 1 are the front and side views of Nc, and parts c and d of Figure 1 are the front and side views of SnNc. Nc has a planar geometry (D_{4h}) while SnNc has a nonplanar geometry (C_{4v}) like an umbrella top. Day et al. have shown this by density functional theory calculation in the case of tin−phthalocyanine.[21] The nonplanarity in SnNc is due to the comparatively large ionic radius of the tin metal ion within the central cavity of the naphthalocyanine backbone. Figure 2 shows the constant-current topographic adlayer images of Nc and SnNc on a graphite basal plane, respectively. Similar frames are used for the spectroscopic measurements.

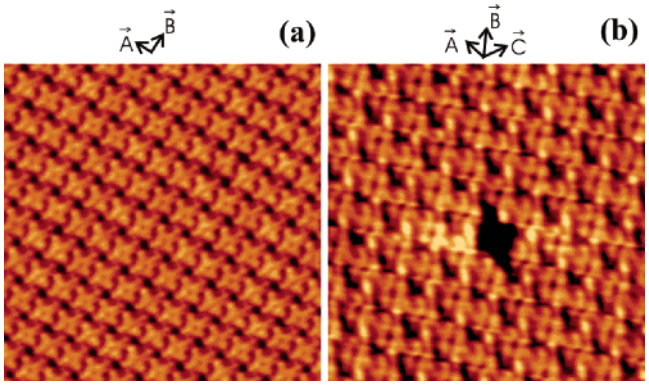

Figure 2. 20 × 20 nm^2 STM constant-current topographic images of Nc (−1.5 V, 0.1 pA) (a) and SnNc (−1.5 V, 1 nA) (b) on graphite (0001). The molecular lattice directions are marked.

Tunneling Spectroscopy of Nc@HOPG. The typical current−voltage characteristics and the normalized differential conductivity−voltage curves of Nc on graphite are given in Figure 3. Current−voltage characteristics are recorded in both voltage ramp directions at different set currents (I_{sp}). Figure 3a shows the current−voltage curves taken at different I_{sp} values. The voltage−ramp direction is from positive to negative, which is referred to as reverse voltage ramp in the following sections. During measurements, the voltage set point (V_{sp}) is kept at 1.35 V. A smaller I_{sp} corresponds to a larger tip−sample distance. A change of I_{sp} from 0 to 300 pA corresponds to a change of approximately 0.3 nm for the tip distance toward the sample. This has been estimated from current−distance characteristics measured during the same experiments. The zero current region between the current offsets is as expected for an adsorbate with a gap between the occupied and unoccupied states in its electronic structure. The $I-V$ curves taken at lower I_{sp} values show a diode-like unsymmetrical nature especially at the negative bias voltage. However, at higher I_{sp} values, the curves are more symmetric in nature. This is due to different tip−molecule and molecule−substrate interfaces and the molecule acting as a diode.[22] That is, when the tip−molecule distance is large, then the tunneling probability of electrons from molecule to tip is less than in the opposite direction and this increases with decreasing tip−molecule distance and hence the tunneling current increases. This supports the idea that the molecules have symmetrical $I-V$ characteristics in general and the asymmetry at lower I_{sp} values arises due to a change in the effective conductivity of the "tip−molecule interfaces".

Figure 3b is the normalized differential conductivity vs voltage of Nc on graphite taken at different I_{sp} values. A particular constant was added to the subsequent curve to lift it above the previous one for a better visualization, and the I_{sp} values corresponding to each curve are given along with the curves. To understand the local density of molecular adsorbates on the surface, the study of differential conductivity, dI/dV, is necessary. But, due to the strong variation in the resonant and elastic intensities with tip−sample separation, it is difficult to identify the local density peaks in the dI/dV curves.[17] Stroscio et al. showed that this difficulty could be eliminated by using

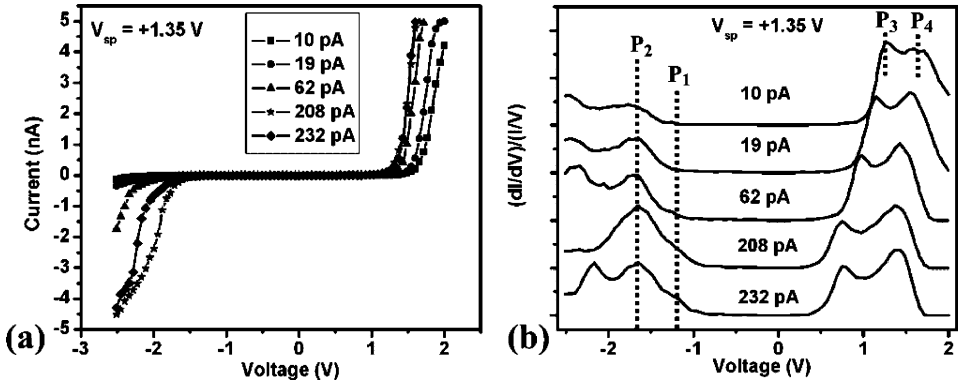

Figure 3. (a) Current−voltage curves of Nc on graphite (0001) and (b) the normalized differential conductivity−voltage characteristics of Nc. V_{sp} is the voltage set point for the corresponding measurements; P_1, P_2, P_3, and P_4 are the peak positions.

TABLE 1: Average Peak Positions of P_1 and P_2, the Peak Positions of P_3 and P_4 at I_{sp} = 10 and 232 pA, and Peak Splitting between P_3 and P_4 at I_{sp} = 10 and 232 pA for the Reverse Voltage Ramp

	average position of P_2	average position of P_1	position of P_3 at I_{sp}		position of P_4 at I_{sp}		splitting between P_3 and P_4 at I_{sp} = 10 pA	splitting between P_3 and P_4 at I_{sp} = 232 pA
			10 pA	232 pA	10 pA	232 pA		
reverse voltage ramp	−1.65 ± 0.05	−1.25 ± 0.05	1.27	0.76	1.63	1.39	0.36 eV	0.63 eV

the logarithmic derivative, d(ln *I*)/d(ln *V*), or normalized differential conductivity, (d*I*/d*V*)/(*I*/*V*), as the spectral intensity function.[23] As expected, the normalized differential conductivity curves of Nc molecules show very distinct peaks corresponding to the electron affinity levels, P_3 and P_4, and the ionization levels, P_1 and P_2, near the Fermi level as shown in Figure 3b. The peak which corresponds to the first ionization level, P_1 (−1.25 ± 0.05 V), starts to appear as a shoulder from I_{sp} at 62 pA. The second ionization level, P_2 (−1.65 ± 0.05 V) which is seen even at very low I_{sp} values, becomes sharp and intense with increasing I_{sp} values. The peak positions are elucidated by a separate Gaussian fitting of these curves. Similar values are shown for the ionization states of Nc using differential conductivity, d*I*/d*V*, in our previous report.[11] The most important point to be noted here is that with the change in I_{sp} there has been no change observed in the positions of P_1 and P_2 within the given experimental accuracy. This means that the ionization levels of the molecules are pinned to the filled band of the substrate. The electron affinity states (P_3 and P_4) show a shift in their relative energy position toward the Fermi energy with increasing I_{sp} (decreasing tip−sample distance). The position of P_3 (1.25 V) and P_4 (1.6 V) at I_{sp} 10 pA can be considered as weakly perturbed electron affinity states since there is the maximum distance between the tip and the molecules. The shift in energy of the first electron affinity level, P_3, is relatively larger compared with that of P_4, that is, an increase in I_{sp} from 10 to 232 pA causes a peak splitting from 0.36 to 0.63 eV between P_3 and P_4. Moreover, the peak intensity corresponding to P_3 is decreased to almost 50%, and a relatively small increase in the intensity for the second electron affinity level, P_4 (8%), is observed. A summary of the peak positions and splitting is given in Table 1.

Numerical averages of (d*I*/d*V*)/(*I*/*V*) curves taken in the reverse (solid curve) and forward (dotted curve) voltage ramp are shown in Figure 4a. The numerical averages show distinct peak positions for P_2 and P_1 (ionization levels), which are −1.65 ± 0.05 and −1.25 ± 0.05 V, respectively, in both curves. The discrepancies in the intensity of peaks in different curves are due to the better response of electronics at the negative voltage part of the curve when the measurements start from a negative voltage and vice versa in the given acquisition time. However, the relative peak intensity ratios are approximately the same in both curves. The differential conductivity is the measure for the LDOS of molecules near Fermi energy. Therefore, it has been compared with theoretically calculated DOS for single molecules. The DOS is shown as a bar diagram in Figure 4a, and the calculations are done using a Gaussian package with a

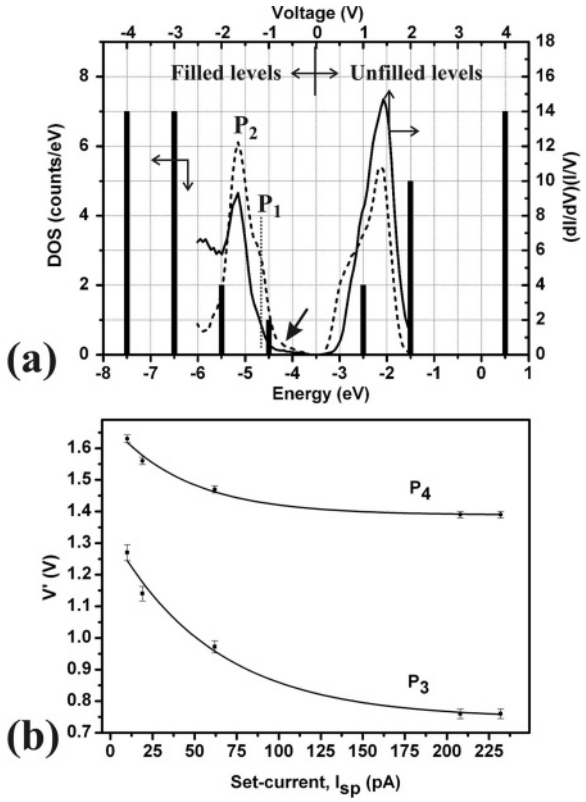

Figure 4. (a) Numerical average of normalized differential conductivity vs voltage taken at different current set points in both voltage ramp directions. The solid line represents the reverse voltage ramp, and the dotted line represents the forward voltage ramp. The bar diagram is the calculated DOS as a function of energy for a single Nc molecule using B3LYP/631G. (b) Plots of the positions (V') of P_3 and P_4 at different current set points (I_{sp}) for the reverse voltage ramp.

TABLE 2: Fitting Parameters V_0', V_1, and I_1 of Curves P_3 and P_4 in Figure 4b

	V_0' (eV)		V_1		I_1		$V_0' + V_1$ at $I_{sp} = 0$ (absolute value of P_3, P_3^0)	$V_0' + V_1$ at $I_{sp} = 0$ (absolute value of P_4, P_4^0)
	P_3	P_4	P_3	P_4	P_3	P_4		
reverse voltage ramp	0.75	1.39	0.59	0.29	60	45.5	1.34 eV	1.68 eV

B3LYP/6-31G basis set. The DOS was calculated by taking the number of states per one electronvolt to best fit the theory and experiment. Zero energy in the bar diagram corresponds to the vacuum level of the Nc molecule, and the zero voltage in the differential conductivity curve is the Fermi level of the molecular adlayer. The midpoint of the HOMO and LUMO in the calculation is assigned as the Fermi energy of single molecules, which is compared with the zero voltage in the experiment. The first local density of the filled level, which is appearing as a shoulder in the experiments, can be correlated with the first ionization level or HOMO of the molecules. Furthermore, the second intense peak in the experiment is attributed to the second local density occupied with two states. This is reasonable due to the double intensity of the second peak (P_2) compared with the first peak (P_1). The calculated local density of unfilled levels shows, however, a discrepancy with the experiments. This is explained by two facts: First it is well-known that the energy positions of the unoccupied levels are not correct in the ab initio methods because there are no electrons in these states. The second is due to the fact that the unfilled states are perturbed due to the tip−molecule interaction and change their position with changing I_{sp}. Therefore, the absolute values of P_3 and P_4 are difficult to conclude from the averaged curve due to the shift in position with I_{sp}. Figure 4b is a plot of the shift in the peak positions of P_3 and P_4 with respect to the set current. The plot is used to find the peak position at zero I_{sp}, which corresponds to the unperturbed peak position (absolute values). The plots are fitted with an exponential decay (solid lines) curve which is given by, $V' = V_0' + V_1 * e^{(-I_{sp}/I_1)}$, where V_0' is the residual potential (V' at infinite I_{sp}) and V_1 and I_1 are constant. Applying the boundary condition, $I_{sp} = 0$, in the above equation gives the absolute peak positions, P_3^0 and P_4^0 (indexed in Table 2). This value provides the absolute HOMO−LUMO gap of the molecule, which is further calculated as 2.59 ± 0.05 eV. However, this value is relatively higher compared with the electronic gap in bulk crystals of metal-free phthalocyanine (2.0−2.2 eV).[24,25] This may be explained by the broadening of single-molecular degenerate levels to a band structure in the bulk crystal. The fitting parameters V_0', V_1, and I_1 for P_3 and P_4 are also given in Table 2. The first peak P_3 is assigned to the theoretically observed first two unfilled levels, which are closely spaced in energy (140 meV), and the second peak P_4 is assigned to the next five unfilled levels. Another interesting observation in the averaged curves is a slow increase in the conductivity below zero voltage (an arrow points the region), which shows a nonvanishing DOS near the Fermi level that is presumably a contribution from the graphite substrate. However, the conductivity increases very sharply above zero voltage.

Tunneling Spectroscopy of SnNc@HOPG. To understand this phenomenon in detail, we have performed the same experiments with nonplanar SnNc, where a much stronger molecule−substrate interaction is expected. A strong molecule−substrate interaction has been found in this case from the adsorption geometry as concluded in the first part of this article (the previous article). The tip−sample distance-dependent current−voltage characteristics and the normalized differential conductivity vs voltage are plotted in Figure 5. The current−voltage curve shows a similar diode-like characteristic as in the case of Nc. However, a steeper increase of the tunneling current is observed, which is attributed to a better conductivity at the SnNc−substrate interface compared with the Nc−substrate interface. The normalized differential conductivity shows no HOMO−LUMO gap shrinking with decreasing tip−sample distance compared with Nc molecules. The states corresponding to electron affinity and ionization levels are pinned onto the substrate DOS. The first ionization level is marked as P_1 (−1.11 ± 0.06 V), and the first and the second electron affinity levels are marked as P_2 (1.18 ± 0.02 V) and P_3 (1.85 ± 0.08 V). The first electron affinity and ionization levels are used to calculate the HOMO−LUMO gap (2.29 ± 0.08 eV). This gap is approximately 300 meV less than that of Nc and shows a more semiconducting behavior of SnNc presumably due to the metal ion. The experimentally observed transport gap is comparable with the reported values of other different metal phthalocyanines such as CuPc (2.2 eV),[24,25] NiPc (2.6 eV),[24,25] and SnPc (2.3 eV)[26] for their bulk crystals.

Figure 6 is the numerical average of normalized differential conductivity−voltage curves taken at different current set points in both voltage ramp directions. The solid curve is taken in the reverse ramp and the dotted curve for the forward voltage ramp; P_1, P_2, and P_3 are the peak positions. The bar diagram is the calculated DOS for a single SnNc molecule using B3LYP/LANL2DZ. The DOS is calculated by taking the number of states per 0.75 eV to best fit the theory and experiment. The first peak in the experiment (P_1) is attributed to the first ionization level (HOMO) below the Fermi energy. The sharp increase in the intensity after the first peak (P_1) is in good agreement with the increase in the density of states in the

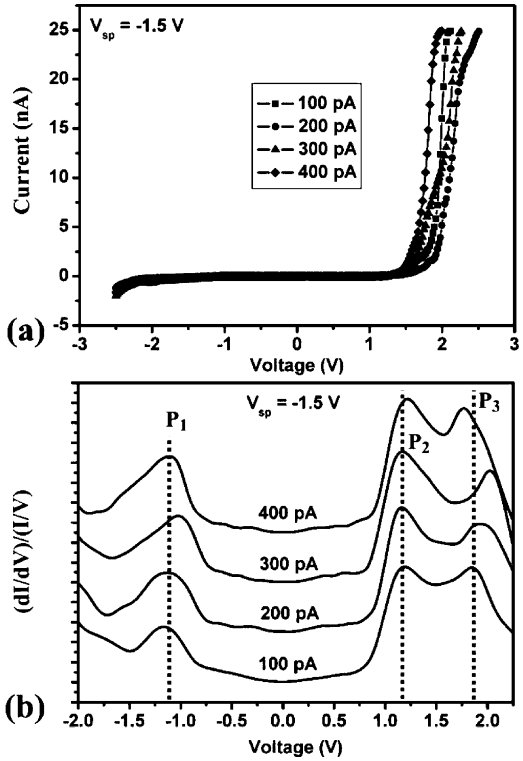

Figure 5. (a) Current−voltage curves and (b) normalized conductivity−voltage characteristics of SnNc on graphite (0001). V_{sp} is the voltage set point for the corresponding measurements. P_1, P_2, and P_3 are the peak positions.

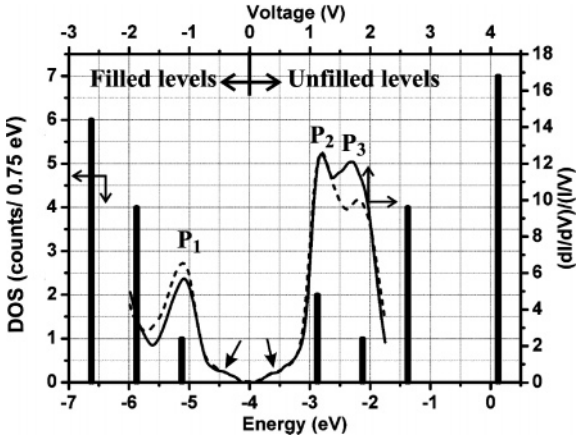

Figure 6. Numerical average of the normalized differential conductivity vs voltage taken at different I_{sp} values. The solid line represents the reverse voltage ramp, and the dotted line represents the forward voltage ramp; P_1, P_2, and P_3 are the peak positions. The bar diagram is the calculated DOS for a single SnNc molecule using B3LYP/LANL2DZ.

calculation. Similarly, the first electron affinity peak (P_2) is attributed to the degenerate LUMOs and the second peak (P_3) to the third unfilled single level. The relative intensity values between P_2 and P_3 show a good agreement with the theoretical calculation. Moreover, a slow increase in the conductivity is observed above and below zero volts before the conductivity sharply increases (the molecular states). These regions are indicated using arrows, and the low DOS is attributed again to the substrate contribution.

Discussion

The relative shift in the position of the first and the second electron affinity peaks in the Nc adlayer with respect to the Fermi level with different I_{sp} is understood by a qualitative model. The tip−molecule and molecule−substrate interfaces and the parameters which are necessary to model the system are shown in Figure 7a. The distance between the tip and molecule is d_{TM}, which is a variable and can be set according to different I_{sp} values. The distance between molecule and substrate is d_{MS}, which is a constant at a given molecule−substrate interface. The transmission probability (T_p) between both tip−molecule and molecule−substrate interfaces strongly depends on the distance, which can be described by $T_p \propto \exp^{-(kd)}$, that is, when the distance between the surfaces is small, the transmission probability is large and vice versa. T_p is a constant between the molecules and the substrate since d_{MS} is a constant. The transmission rate of electrons into the molecule becomes greater than the transmission rate between the molecule−substrate interface, when d_{TM} is smaller than a critical value. This increase in the transmission rate causes the electrons to reside in the molecules for a short time (residual time). This residual time of the electron in the system can be defined by the nature of molecule−substrate interface. That is, if the interface has more capacitive character, then the electrons have a longer residual time compared with that in a pure resistive interface. Thus, in a capacitive interface, electrons partially fill the unfilled levels near the Fermi energy and charge the molecules partially. The charging causes a lowering of energy of these low-lying unfilled levels compared with the uncharged molecules.[17] Thus, the shift of the first and second electron affinity peaks to lower energy when the tip−sample distance is lowered in the case of the Nc adlayer can be modeled by a pure capacitive Nc−graphite interface and SnNc−graphite interface as purely ohmic. The electronic equivalents of the molecule−substrate interface in both SnNc and Nc cases are sketched in Figure 7b. In a practical case, these electronic equivalents of different interfaces are assigned in terms of a molecule−substrate interaction, that is, Nc molecules have a weak molecule−substrate interaction (capacitive interface) and SnNc have strong molecule−substrate interaction (ohmic interface).

From the previous discussion, one can now define the physical significance of the parameters used to fit the exponential shift of the first and second local density of unfilled levels, which is indexed in Table 2. The exponential behavior of the shift shows that there is a limiting value for the tip-induced charging of molecules defined as the residual potential (V_0'). The sum of V_0' and the constant V_1 at zero I_{sp} corresponds to the unperturbed (absolute value, P_n^0) electron affinity levels. The difference between the absolute value (P_n^0) of an electron affinity level to V_0' is equal to the charging energy (E_c), the shift in energy position of an unoccupied level when it is at a maximum charge. The smaller decay constant (I_1, given in Table 2) corresponding to the second local density peak of unfilled levels shows that the charging of these levels with the decreased tip−sample distance is smaller compared with that of the first. This is reasonable, according to the occupation (Aufbau) principle in which the lower energy levels are populated first and then the second level and so on. Due to the small energy difference between the first two unfilled levels (140 meV), the electrons fill these two levels first and then proceed to the third level and so on. The decrease in intensity of the first electron affinity level's peak is presumably due to the change in tunneling probability caused by the change in position of these levels from the voltage set value (orbital-mediated tunneling) induced by the tip−sample distance. The small increase in the intensity of the second electron affinity level's peak can be explained by a similar effect, where the tunneling probability increases due to the alignment of these levels close to the voltage set value.

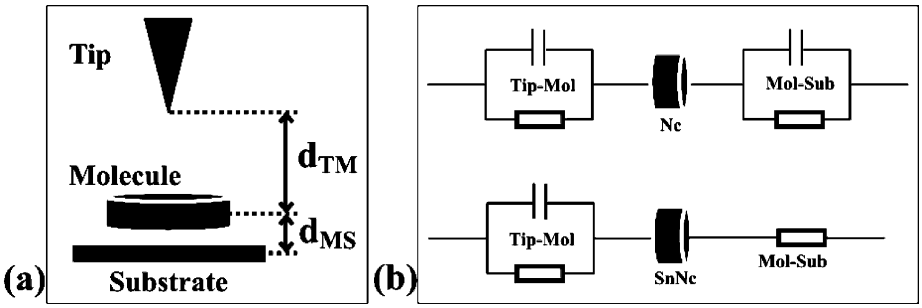

Figure 7. (a) Schematic representation of tip−molecule and molecule−substrate interfaces and the geometric distances at these interfaces. (b) The electronic equivalents of tip−molecule (Tip−Mol) and molecule−substrate (Mol−Sub) interfaces in Nc and SnNc.

Conclusion

Tip−sample distance-dependent current−voltage characteristics have been measured at Nc−graphite and SnNc−graphite interfaces. Both show a diode-like nature at large tip−sample distances. Normalized differential conductivity−voltage curves are characterized and compared with the theoretically calculated density of states. The HOMO−LUMO gap for Nc is calculated from the first electron affinity and ionization levels, 2.59 ± 0.05 eV, and found to be approximately 300 meV larger compared with that of SnNc. The low HOMO−LUMO gap in SnNc is due to the metal ion, which makes the molecule more semiconducting at the substrate. Nc molecules show a tip−sample distance-dependent HOMO−LUMO gap shrinking. The filled levels are found pinned onto the graphite substrate filled levels; however, the unfilled levels near the Fermi level show a shift in their position with decreasing tip−sample distance. This shift is assigned to the charging of these levels during the tunneling process which is caused by a weak molecule−substrate interaction. This interface is then modeled as a capacitive electronic equivalent interface. Due to the strong molecule−substrate interaction, in SnNc the normalized differential conductivity−voltage curves however show no HOMO−LUMO gap shrinking or charging of the unfilled levels. The interface is assigned in this case to a pure ohmic interface.

Acknowledgment. T.G.G. thanks the "Deutsche Forschungsgemeinschaft" for financial support within the Graduate College "Accumulation of Single Molecules to Nanostructures".

References and Notes

(1) Coldren, L. A.; Corzine, S. W. *Diode Lasers and Photonic Integrated Circuits*; John Wiley: New York, 1995.

(2) Miller, D. A. B.; Chemla, D. S.; Damen, T. C.; Gossard, A. C.; Wiegmann, W.; Wood, T. H.; Burrus, C. A. *Phys. Rev. B* **1985**, *32*, 1043.

(3) Lam, J. F.; Forrest, S. R.; Tangonan, G. L. *Phys. Rev. Lett.* **1991**, *66*, 1614.

(4) So, F. F.; Forrest, S. R. *Phys. Rev. Lett.* **1991**, *66*, 2649−2652.

(5) Leznoff, C. C., Lever, A. B. P., Eds. *Phthalocyanines: Properties and Applications*; VCH Publishers: New York, 1989.

(6) Wang, D. X.; Tanaka, Y.; Iizuka, M.; Kuniyoshi, S.; Kudo, K.; Tanaka, K. *Jpn. J. Appl. Phys.* **1999**, *38*, 256−59.

(7) Spadavecchia, J.; Ciccarella, G.; Stomeo, T.; Rella, R.; Capone, S.; Siciliano, P. *Chem. Mater.* **2004**, *16*, 2083−2090.

(8) Uchida, S.; Xue, J. Rand, B. P.; Forrest, S. R. *Appl. Phys. Lett.* **2004**, *84*, 4218−20.

(9) Barlow, D. E.; Hipps, K. W. *J. Phys. Chem. B* **2000,** *104*, 5993−6000.

(10) Walzer, K.; Hietschold, M. *Surf. Sci.* **2001**, *471*, 1.

(11) Lackinger, M.; Müller, T.; Gopakumar, T. G.; Müller, F.; Hietschold, M.; Flynn, G. W. *J. Phys. Chem. B* **2004**, *108*, 2279.

(12) Alvarado, S. F.; Rossi, L.; Muller, P.; Riess, W. *Synth. Met.* **2001**, *122*, 73−77.

(13) Hipps, K. W.; Barlow, D. E.; Mazur, U. *J. Phys. Chem. B* **2000,** *104*, 2444−2447.

(14) Mazur, U.; Hipps, K. W. *J. Phys. Chem.* **1994**, *98*, 8169−8172.

(15) Mazur, U.; Hipps, K. W. *J. Phys. Chem. B* **1999**, *103*, 9721−9727.

(16) Qiu, X. H.; Nazin, G. V.; Ho, W. *Phys. Rev. Lett.* **2004**, *92*, 206102.

(17) Deng, W.; Hipps, K. W. *J. Phys. Chem. B* **2003**, *107*, 10736−10740.

(18) McEllistrem, M.; Haase, G.; Chen, D.; Hamers, R. J. *Phys. Rev. Lett.* **1993**, *70*, 2471−2474.

(19) Feenstra, R. M. *Phys. Rev. B* **1994**, *50*, 4561.

(20) Müller, A.-D.; Müller, F.; Hietschold, M. *Appl. Phys. Lett.* **1999**, *74*, 2963.

(21) Day, P. N.; Wang, Z.; Pachter, R. *J. Mol. Struct. (THEOCHEM)* **1998**, *455*, 33−50.

(22) Larade, B.; Bratkovsky, A. M. *Phys. Rev. B* **2003**, *68*, 235305.

(23) Stroscio, J. A.; Feenstra, R. M.; Fein, A. P. *Phys. Rev. Lett.* **1986**, *57*, 2579.

(24) Turek, P.; Petit, P.; Andre, J. J.; Simon, J.; Even, R.; Boudjema, B.; Guillaud, G.; Maitrot, M. *J. Am. Chem. Soc.* **1987**, *109*, 5119−5122.

(25) McKeown, N. B. *Phthalocyanine Materials: synthesis, structure and function*; Cambridge University Press: Cambridge, U.K., 1998.

(26) Cabailh, G.; Wells, J. W.; McGovern, I. T.; Dhanak, V. R.; Vearey-Roberts, A. R.; Bushell, A.; Evans, D. A. *J. Phys.: Condens. Matter* **2003**, *15*, S2741−S2748.